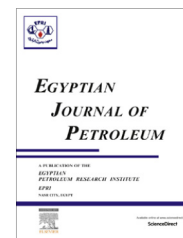




Egyptian Petroleum Research Institute
Egyptian Journal of Petroleum

www.elsevier.com/locate/egyjp
www.sciencedirect.com



FULL LENGTH ARTICLE

Application of seismic attributes in structural study and fracture analysis of DQ oil field, Iran



Shahoo Maleki ^{a,*}, Hamid Reza Ramazi ^a, Raof Gholami ^b, Farhad Sadeghzadeh ^c

^a Department of Mining and Metallurgy Engineering, Amirkabir University of Technology (Tehran Polytechnic), Tehran, Iran

^b Department of Chemical and Petroleum Engineering, Curtin University, Sarawak, Malaysia

^c Drilling Division, Arvandan Oilfield Company, Ahwaz, Iran

Received 22 October 2013; accepted 26 February 2014

Available online 15 June 2015

KEYWORDS

Seismic attributes;
Fracture analysis;
Structural study;
Stability

Abstract The determination of the most unstable areas in oil fields is critical for addressing engineering problems of wellbore and sand production as well as geologic problems such as understanding dynamic constraints on hydrocarbon migration and fracture permeability. In this research work, coherency seismic attribute has been used for the determination of the most critical areas in terms of drilling stabilities in the DQ oil field, Iran. The results obtained have shown that the (1) predominant features are the SSE–NNW and N–S trends (2) the central part of the DQ structure shows the highest concentration of segment bundles, (3) the segment bundles seem to be aligned along some lineaments oriented SE–NW and SSE–NNW, and (4) on the eastern and western margins of the map there is an anomalous concentration of segments oriented E–W. It can be concluded that coherency attribute is a valuable tool for structural analysis highlighting those areas containing unstable features.

© 2015 The Authors. Production and hosting by Elsevier B.V. on behalf of Egyptian Petroleum Research Institute. This is an open access article under the CC BY-NC-ND license (<http://creativecommons.org/licenses/by-nc-nd/4.0/>).

1. Introduction

Tensile and shear failure are the major mechanisms resulting in borehole instability problems such as blowout, lost circulation, stuck tools and collapse of borehole. The complicated accidents caused by borehole instability give rise to serious drilling quality and safety problems. More than six billion dollars are spent in controlling borehole instability in the global petroleum industry every year. For achieving safe, high quality

and highly efficient drilling, it is vital to understand properly and estimate effectively the stress state of enclosing rock of borehole, explore mechanisms of borehole instability and establish prediction theory of borehole stability.

Analyzing borehole stability through rock mechanics theory is a major way to research on borehole stability [1–5]. Many accurate ways have been found to determine petrophysical, elastic and strength parameters of formation via seismic and well log data [6]. Based on the above parameters, the stress state of the enclosing rock of the borehole can be analyzed and calculated through the mechanics theory of the porous medium and the calculation model of the in situ stress.

Conventional researches on borehole stability are usually carried out after drilling, which can help determine the major

* Corresponding author.

E-mail address: Sh.maleki.ch@gmail.com (S. Maleki).

Peer review under responsibility of Egyptian Petroleum Research Institute.

<http://dx.doi.org/10.1016/j.ejpe.2015.05.001>

1110-0621 © 2015 The Authors. Production and hosting by Elsevier B.V. on behalf of Egyptian Petroleum Research Institute. This is an open access article under the CC BY-NC-ND license (<http://creativecommons.org/licenses/by-nc-nd/4.0/>).

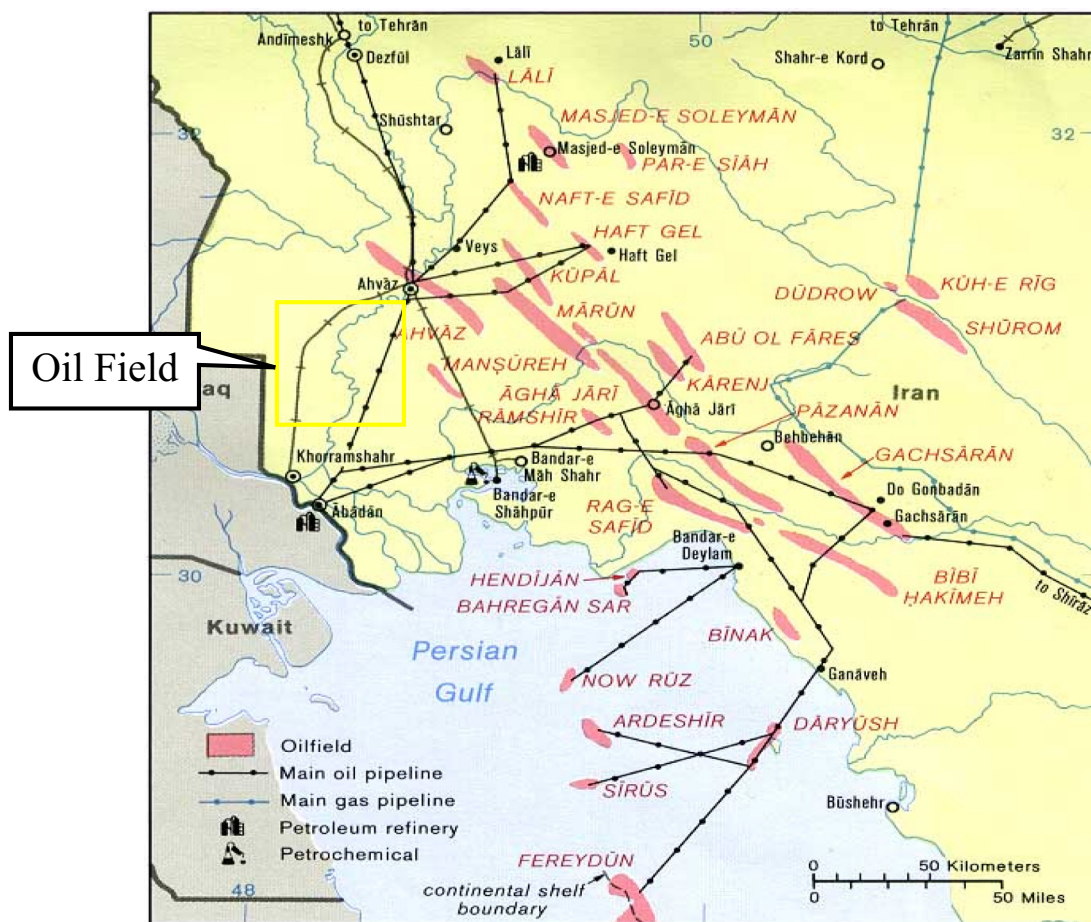


Figure 1 Geographical location of oil field.

mechanism of borehole instability, propose improvement measures and guide succeeding drilling through comprehensive analysis of drilling, well log and core data. However, from the perspective of engineering practicality, borehole instability problems must be predicted in advance, found at the earliest possible time and solved as soon as possible. Meanwhile, because of the deficiency of available information, the pre-drilling prediction is a difficult frontier technology, in which major resources available are seismic data of prospecting area and well log and test data of offset wells. In this regard, the research on borehole stability prediction before drilling is of great significance.

A methodology for determining the orientation and relative magnitude of crustal stresses is now well-established (e.g., [7–9]) and has been utilized at literally thousands of sites, e.g., [10]. In many research works, it has been shown that fractures and faults play an important role in controlling the strength properties of rocks but not all of them are equally important for failure and deformation processes. In situ stresses, at depth, including orientation and magnitude, have a dominant effect on well completion and production processes. In this regard, the issue of wellbore stability has gained particular importance in the last 10 years as a response to the increase in the exploration of complex areas which represent major engineering challenges in drilling and production [11].

A seismic attribute is a quantitative measure of a seismic characteristic of interest. An analysis of attributes has been

integral to reflection seismic interpretation since the 1930s when geophysicists started to pick travel times to coherent reflections on seismic field records [12]. There are now more than 50 distinct seismic attributes calculated from seismic data and applied to the interpretation of geologic structure, stratigraphy, and rock/pore fluid properties [13]. The coherency attribute is a mathematical measure of similarity between adjacent seismic traces. The coherence cube calculated on 3D seismic presents similarity (or dissimilarity) of the seismic waveforms, and hence in what the seismic waveforms represent. That is, coherence cube processing reveals shapes of subsurface reflectors such as pinchouts, unconformities, and channel boundaries, and subtle sedimentological features that are difficult to interpret on traditional seismic volumes [14]. Hence, the aim of this paper is to use seismic attributes, more specifically coherency attribute, for fracture analysis and determination of the most critical areas for drilling program in the DQ oil field, Iran.

2. Study area

This study uses the data belonging to an oilfield located in the Iranian Province of Kuzestan, onshore the Ahvaz region, near the Iran–Iraq frontier. The field is a north–south oriented gentle anti-cline, located in the Dezful Embayment, which is a sector associated with the closing of the Neo-Tethys Sea and the Tertiary formation of the Zagros–Taurus Mountains. The oilfield is close to the west of the Basrah area. The structures in

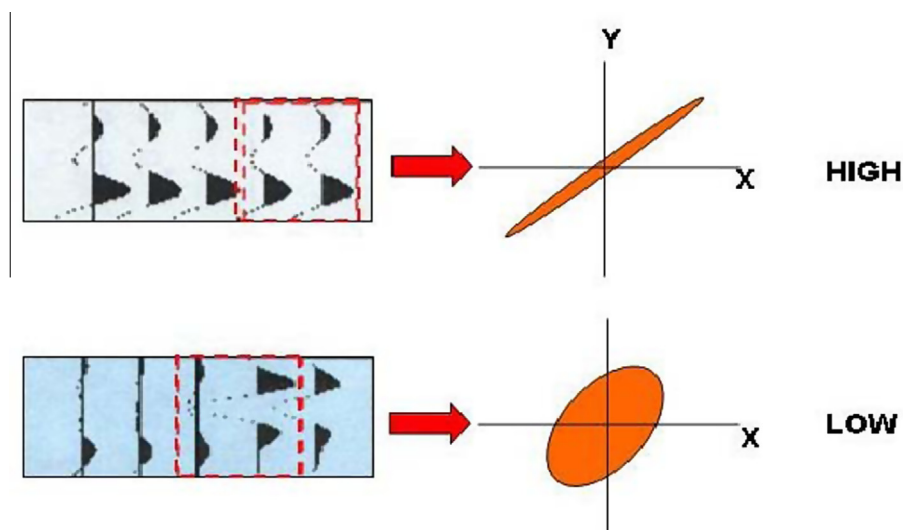


Figure 2 Basic principle of coherency. The clouds of points are an indicator of the similarity of two adjacent well correlated traces. The first ellipse represents a higher continuity between the two adjacent traces than the second ellipse.

Table 1 Vertical analysis window picked for analysis.

Time range (ms)	Windows size (ms)
0–1000	60
1000–2000	90
2000–3000	120

the Basrah area consist of gentle anti-clines showing a north–south general trend which is the same to this field. The trend of these anticlines follows the old north–south oriented basement lines. The presence of Precambrian and early Cambrian salt in the Northern Persian Gulf area and Saudi Arabia is considered as a reason to explain the possible origin of these structures. However, the development of these anticlines seems related to the reactivation of basement faults which can be responsible for their structural evolution. The structural growth of the field area may have already started during the Mesozoic Era or earlier and continue through the time. The Fahliyan formation is well exposed in the Zagros Mountains in Fars Province [15]. At the same time of the sedimentation of the Fahliyan, in the area located between the oilfield and the Khuzestan Province, the intra-shelf basin of the Garau formation takes place. The current oilfield area at the time of the Fahliyan sedimentation must belong to an articulate carbonate ramp complex, partly controlled by local tectonics, partly by sea level changes, probably limited eastward by a more subsiding area that has undergone a deeper sedimentation. Argillaceous limestones and shales of deep environment are also developed offshore Kuwait, suggesting that this area belongs to the same intra-shelf basin. The sedimentation of these units is related to the significant sea level rise that started during the late Tithonian and continued to the early Berriasian [16]. The shallow water sequences of Fahliyan and equivalent units of northern Persian Gulf underlay the shale and bioclastic limestone of the Ratawi formation.

These structures continue southwards to Kuwait showing the same orientation. Fig. 1 shows the geographical location of the DQ oil field in Iran.

3. Seismic and well logs data

The DQ Field is covered by 3D seismic survey acquired by NIOC over an area of about 500 km². The two released final volumes (spike and gapped Deconvolution) were confirmed to be of high quality data. To carry out the following study, a specific post-migration reprocessing was performed. In this regard, Spike Deconvolution, Spectral Whitening, Stratigraphic Deconvolution and Notch dimensional spatial filter in the frequency domain were applied to improve the vertical resolution and to attenuate the acquisition footprint.

Complete well log datasets (including calibrated “compressional” sonic curves) were considered and loaded on Hampson–Russel software in order to study the quantitative relationships between acoustic and litho-petrophysical properties and to support seismic lithology activities (inversion and calibration). At the same time, a set of acoustic and petrophysical curves, including the generated synthetic seismograms, were used to correlate well and seismic information.

4. Seismic attributes

The seismic attributes extracted from pre-stack or post-stack seismic data by mathematical transformations are specific parameters which reflect intrinsic characteristics of seismic wave. Seismic attributes can be used to analyze and predict geologic information because spatial changes of properties of stratigraphic rock and fluid can result in changes of seismic attributes which reflect geometry, kinematics, dynamics, and statistics characteristics of seismic information. Through seismic attribute analysis, the hidden information about lithological, structural, sequential, petrophysical and petroliferous characteristics of formations can be picked up from seismic data so that the potential of seismic data can be explored fully [17–26]. There are many different types of attributes used for geological and petrophysical modeling including instantaneous amplitude, instantaneous phase, instantaneous frequency, root-mean-square amplitude, average absolute amplitude,

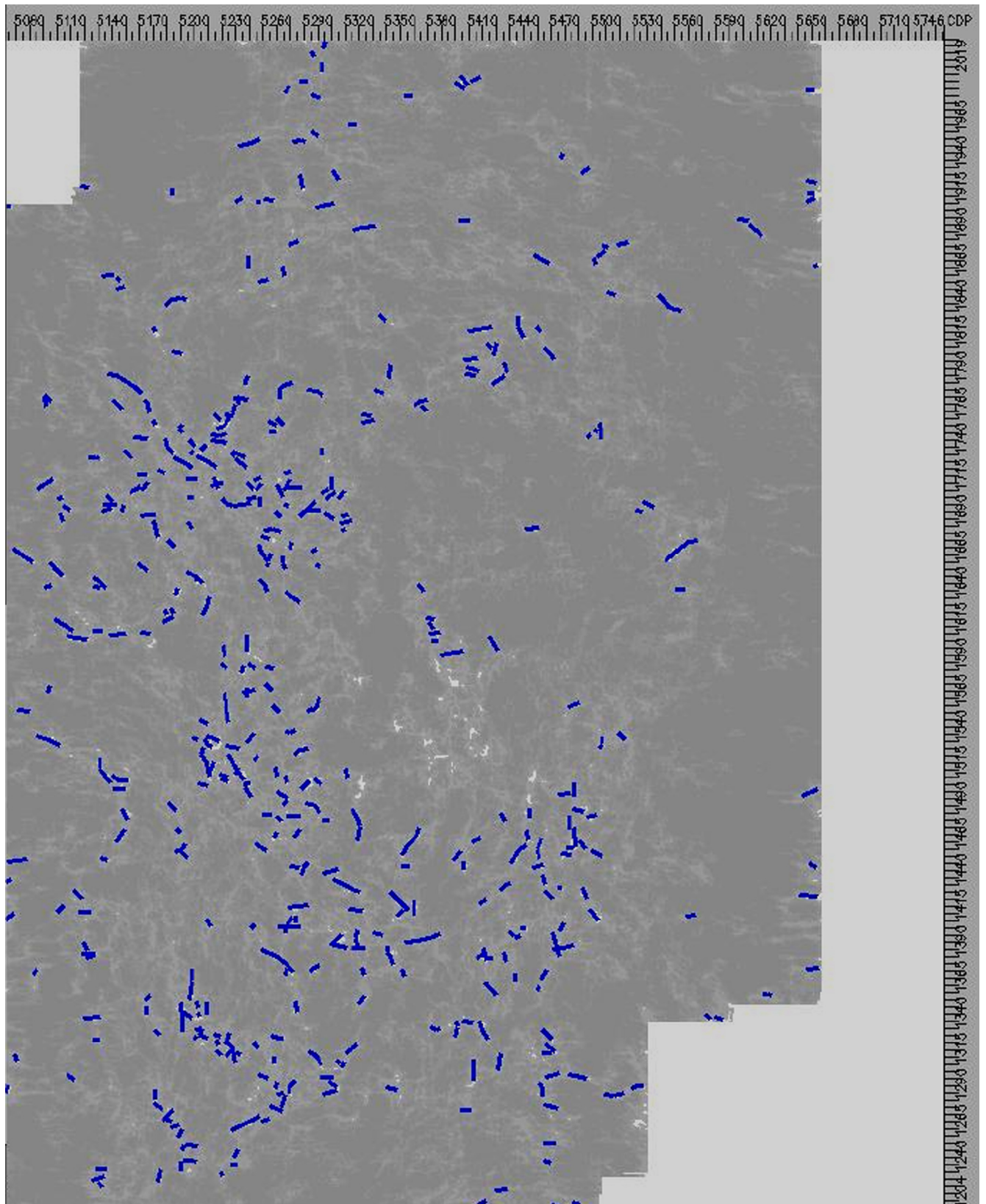


Figure 3 Linear features traced using contrast differences, texture variations and color spectra shifts.

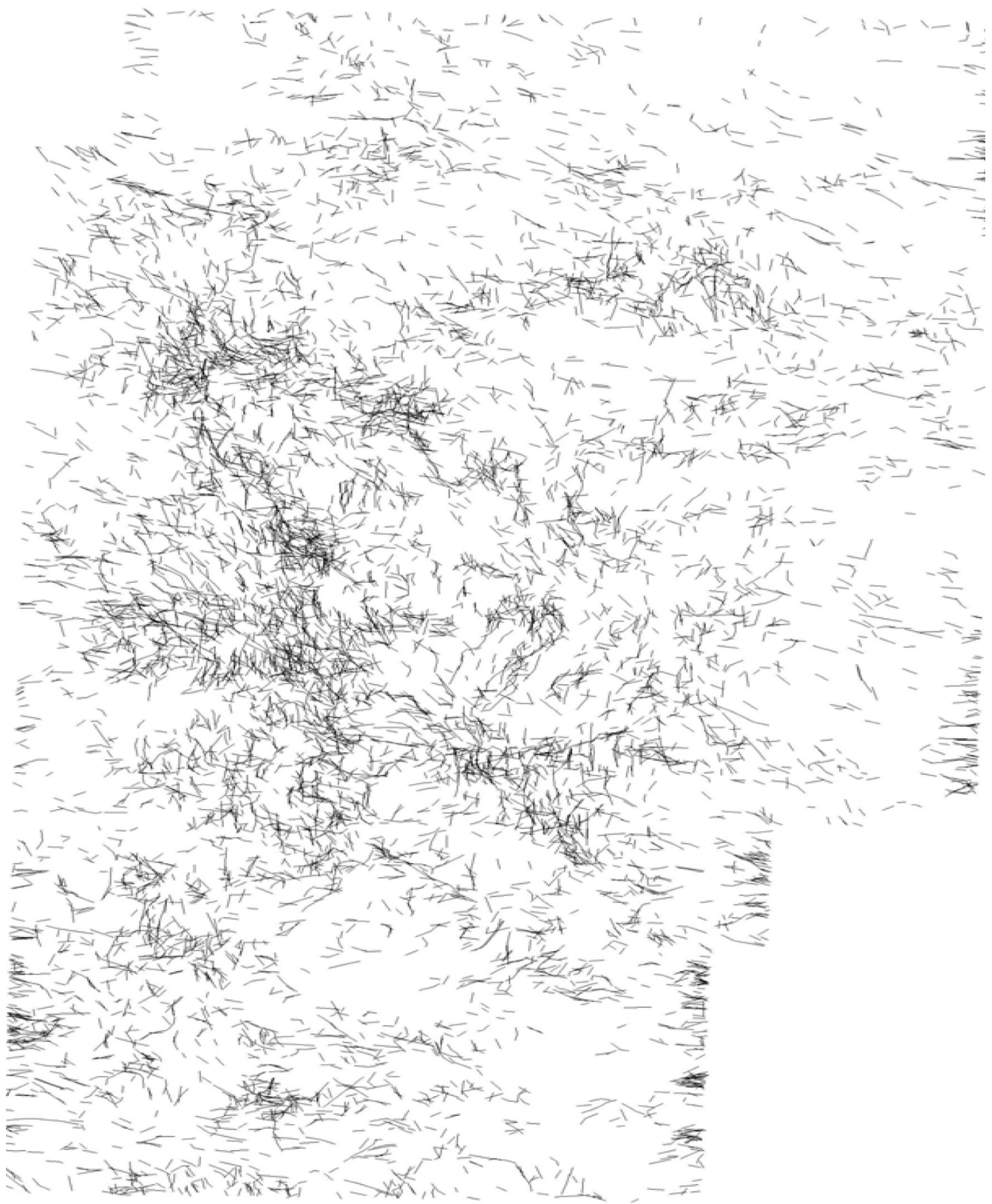


Figure 4 Resulting pattern map comprises 10,670 segments highlighting all lineaments interpreted on the chosen time slices.

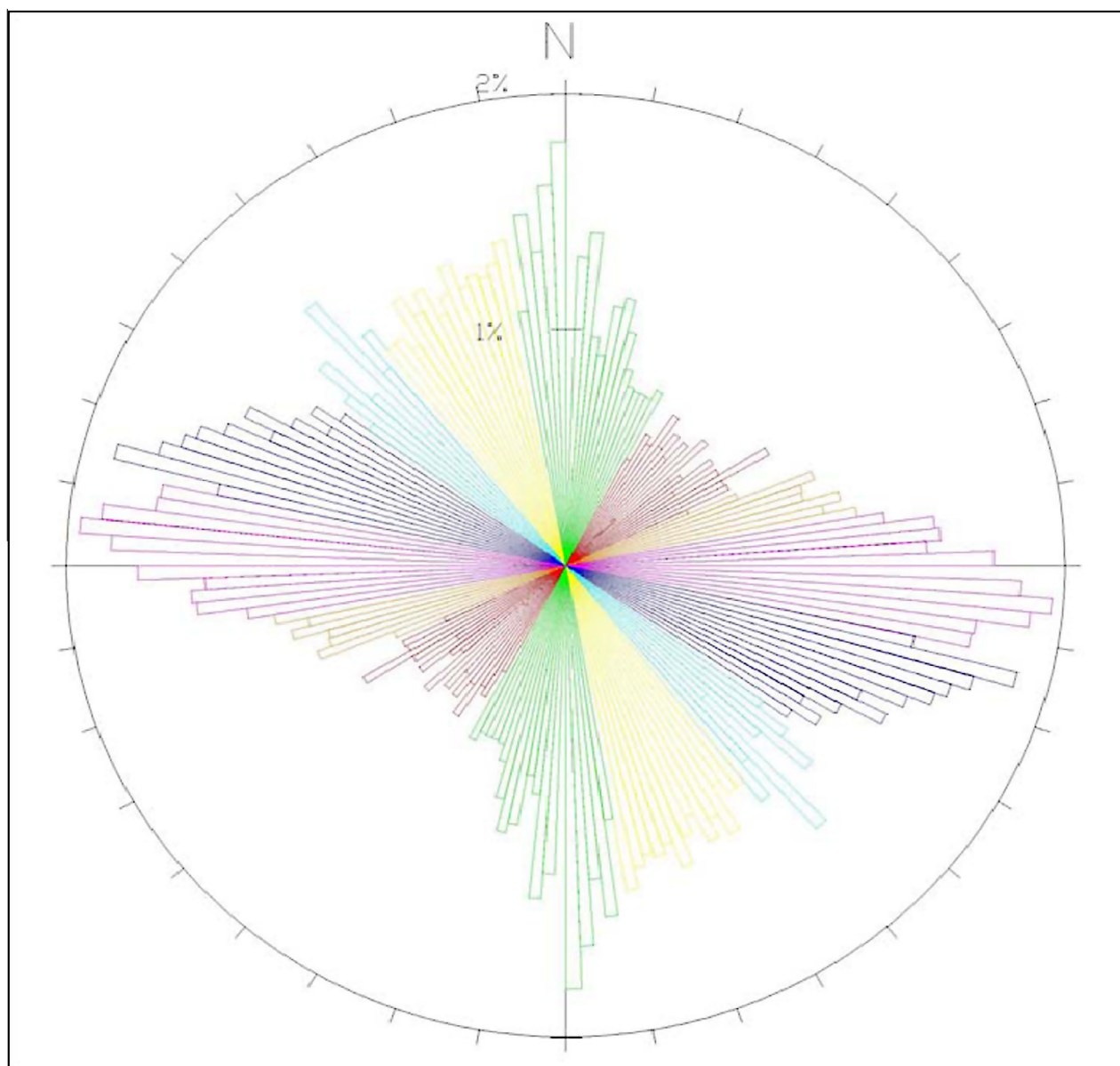


Figure 5 Rosette diagram of the total population, weighted for length of the features. The total numbers of considered segments (10,670) are subdivided into 90 classes (range is 02°). The rosette diagram has highlighted the presence of seven different trends (The main displayed trends are: 350° N– 028° N Trend N–S (green), 028° N– 066° N Trend NE–SW (red), 066° N– 080° N Trend ENE–WSW (orange) 080° N– 102° N Trend E–W (magenta), 0102° N– 126° N Trend ESE–WNW (blue), 0126° N– 142° N Trend SE–NW (cyan), 0142° N– 170° N Trend SSE–NNW (yellow)).

coherency, autoregressive coefficients, etc. Coherency is the one usually used for structural mapping and highlighting faults on seismic volume. Coherence values also announce changes in seismic response due to lithology, or due to spatial changes in rock physical properties such as porosity, pore fluid, permeability, and elastic properties. Specifically, faults and stratigraphic boundaries exhibit the greatest amount of trace-to-trace dissimilarity.

The basic principle of the coherency attribute is exposed in Fig. 2. As shown, if we crossplot the amplitudes of two adjacent well correlated trace snaps, a cloud of much thinner points will be obtained than the one obtained if the two traces were less similar.

Coherency (continuity) is a quantitative measurement of such property, locally computed on a small cube centered on each sample contained in a seismic volume.

In this paper, the seismic attributes used to construct the structural model are extracted from weighted stacking trace of borehole-side seismic traces. In the first place, the time–depth correspondence relationship between seismic and well log data must be determined by acoustic log data or VSP data of drilled wells to calibrate horizons accurately. With the exception of instantaneous attributes, the choice of the size of time-limited moving window has a significant impact on calculating attributes. Practical application indicates the appropriate size range of the time window is 60–120 ms (Table 1).

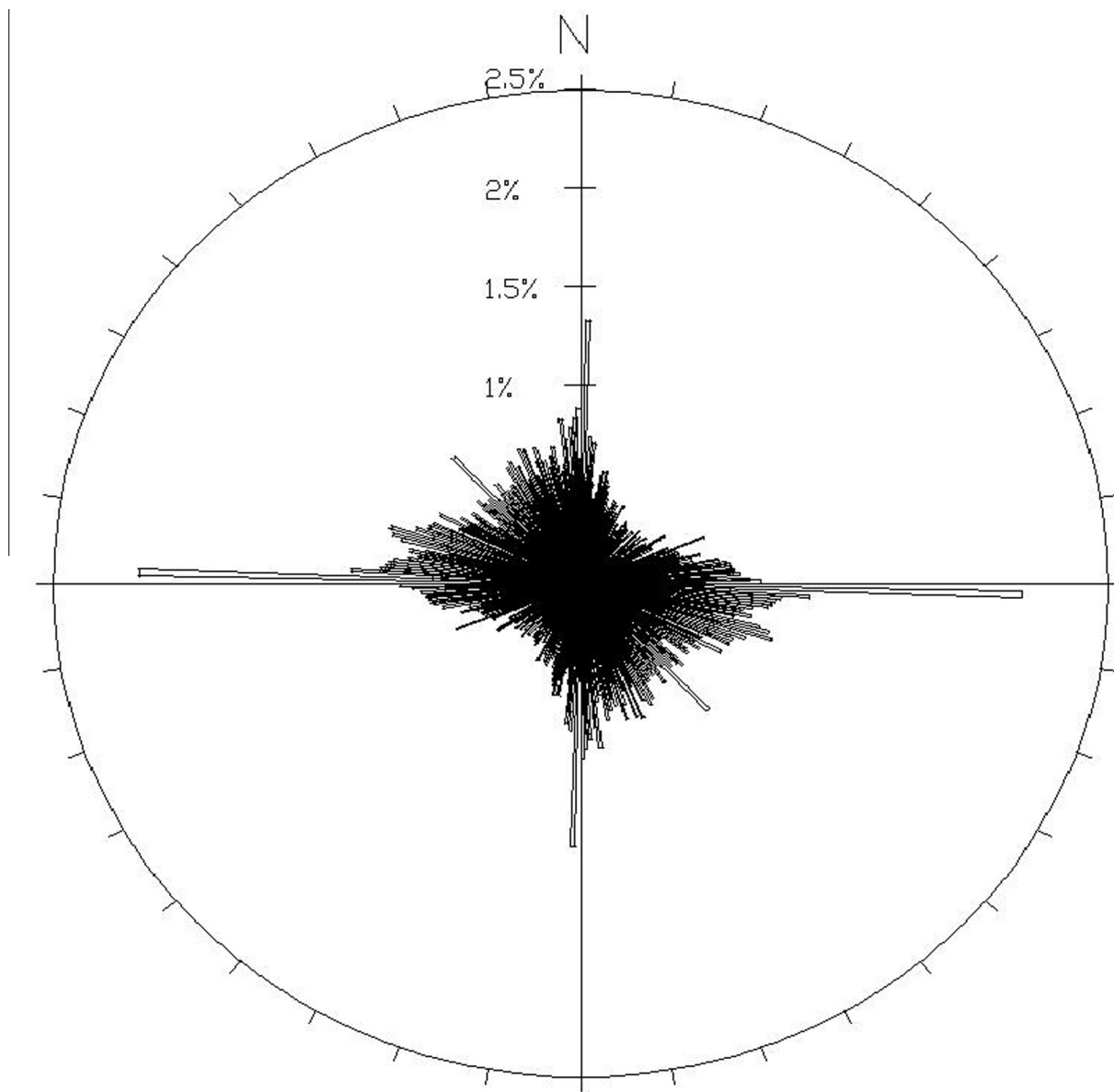


Figure 6 Rosette diagram of the entire segments population, weighted for length of the features, before the application of filtering. The predominant distribution of segments in the classes 000°–002° and 180°–182° due to the seismic acquisition direction (seismic footprint) can be observed.

Table 2 Main trends displayed in the rosette diagram.

Trend	Color
350° N–028° N Trend N–S	Green
028° N–066° N Trend NE–SW	Red
066° N–080° N Trend ENE–WSW	Orange
080° N–102° N Trend E–W	Magenta
0102° N–126° N Trend ESE–WNW	Blue
0126° N–142° N Trend SE–NW	Cyan
0142° N–170° N Trend SSE–NNW	Yellow

In addition, mild dip compensation has been allowed (± 2 samples, with a “dip window” of 90 traces).

5. Fracture analysis

From the entire coherency cube, nineteen time slices have been extracted, sampled every 40 ms between 2200 and 2920 ms. This time window has been chosen to fully cover the time interval characterized by the presence of a Formation named Fahliyan, which represents the reservoir in the DQ structure. Time-slice 2200 ms, time-slice 2240 ms, time-slice 2280 ms, time-slice 2320 ms, time-slice 2360 ms, time-slice 2400 ms, time-slice 2440 ms, time-slice 2480 ms, time-slice 2520 ms, time-slice 2560 ms, time-slice 2600 ms, time-slice 2640 ms, time-slice 2680 ms, time-slice 2720 ms, time-slice 2760 ms, time-slice 2800 ms, time-slice 2840 ms, time-slice 2880 ms, time-slice 2920 ms.

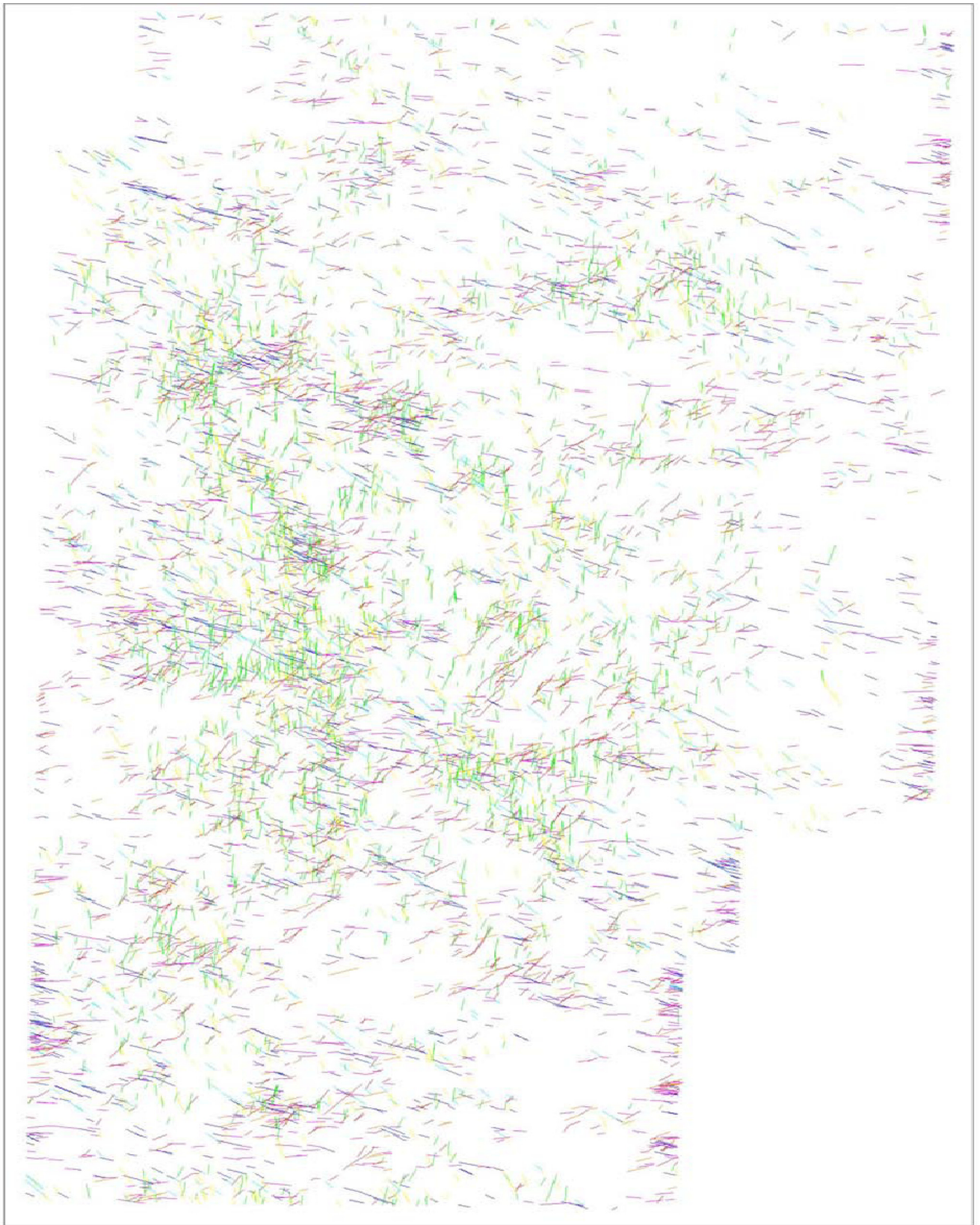


Figure 7 Resulting pattern map after the color coded operation.

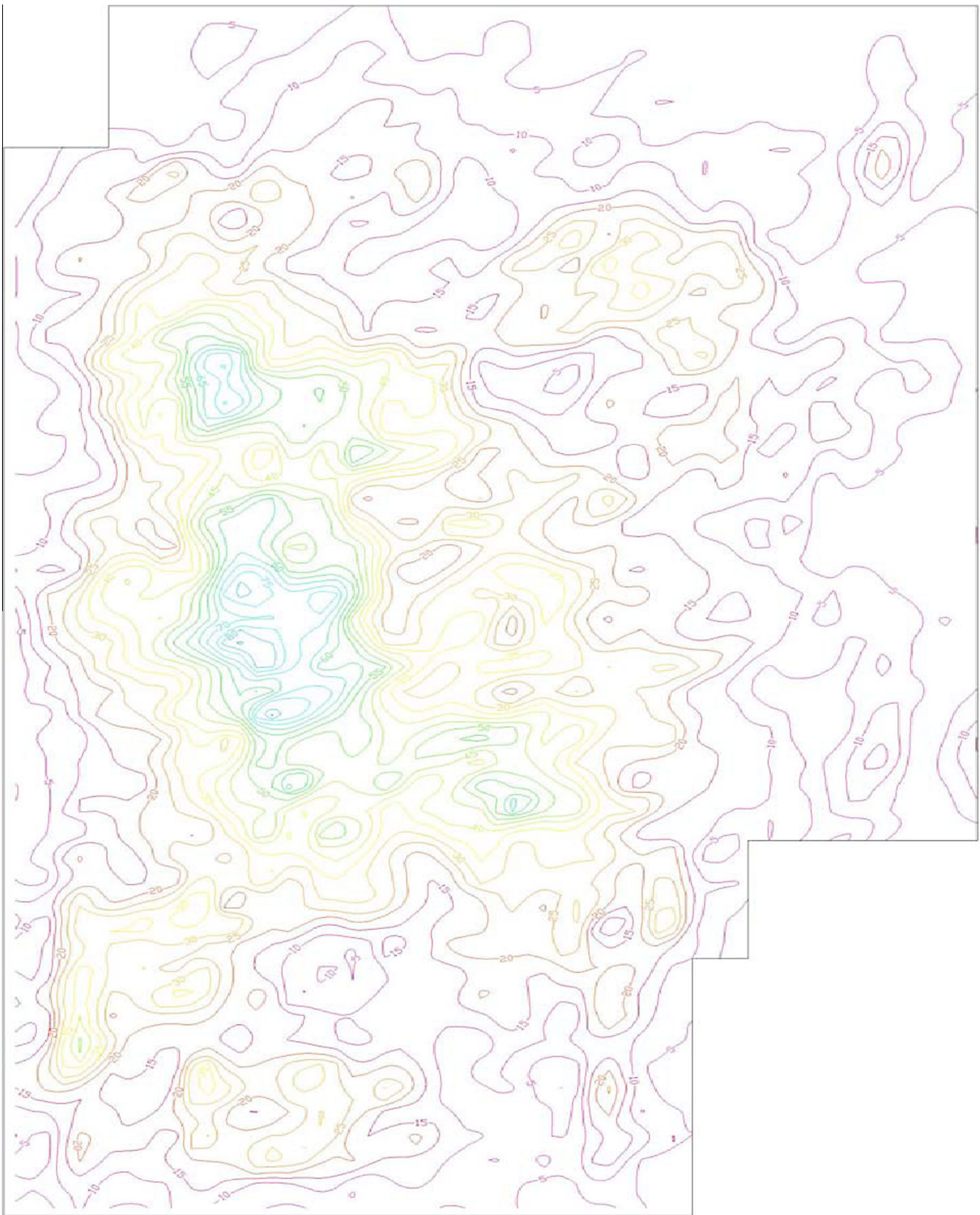


Figure 8 Fracture Potential Contour Map can be interpreted as reflecting the areal variation of fracture potential or total strain.

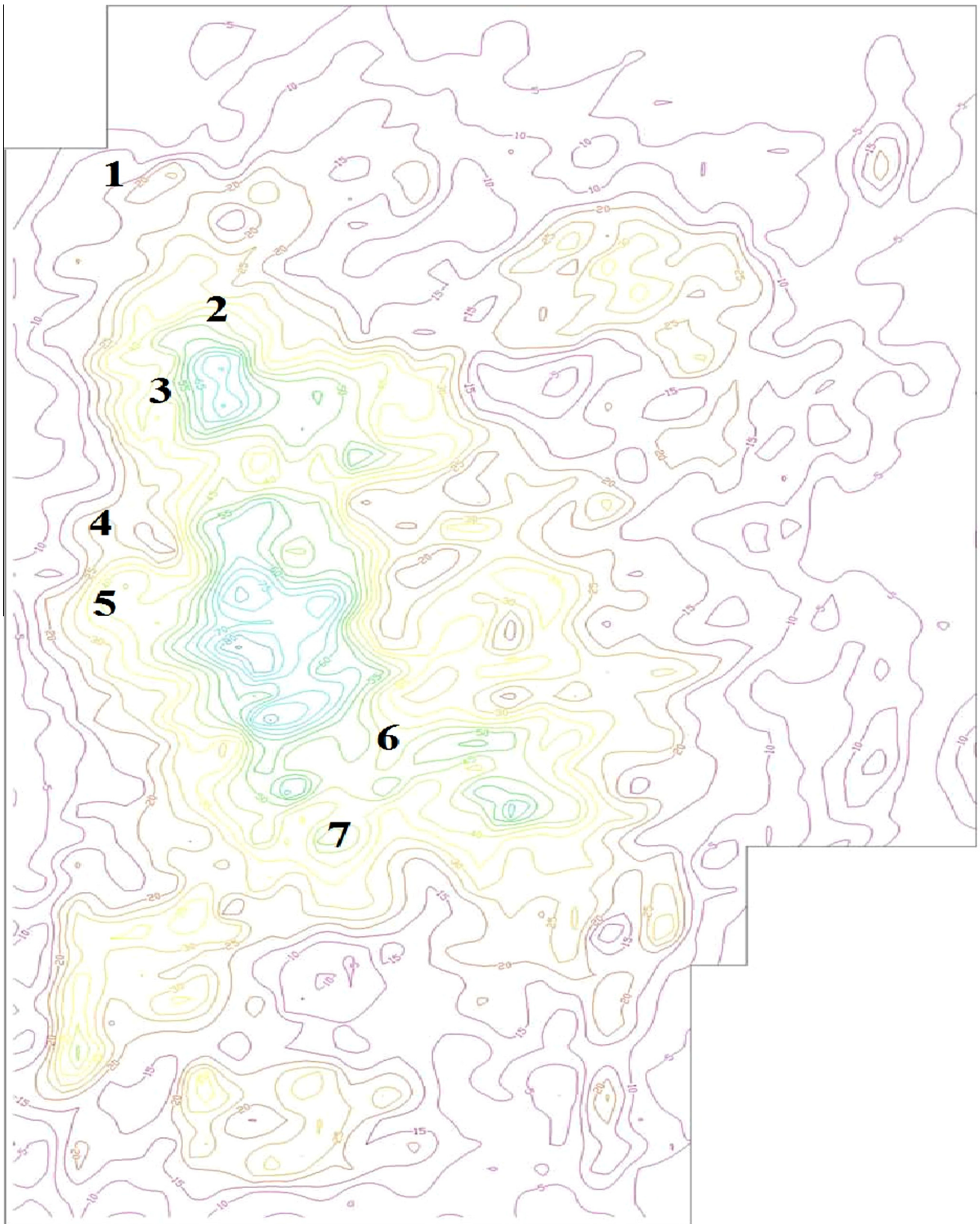


Figure 9 A comparison between the Pattern Map and the Fracture Potential Contour Map. There are some areas of maximum potential that can coincide with the segment bundles.

On each time-slice, linear features (i.e. potential fracture zone) were traced using contrast differences, texture variations and color spectrum shifts (Fig. 3). The interpreted lineaments were subsequently exported to a Geographical Information System (GIS) for geographically linking to a UTM frame.

The resulting pattern map (Fig. 4) comprises 10,670 segments and can be considered as a transparent image of all lineaments interpreted on the chosen time slices. The number of segments considered in this analysis is the result of a filtering operation. In fact, to avoid problems related to the seismic acquisition (possible presence of residual acquisition footprint), the data comprised in the range of 000°–002° and 180°–182° (the seismic acquisition direction) have been not considered in the computation.

The first analysis performed comprises the generation of a rosette diagram for the total population, weighted for the length of the features (Figs. 5 and 6). In the rosette diagram, we consider the main trends recognized. The main displayed trends are given in Table 2.

The analysis of this Rosette diagram shows that lineaments are fairly distributed, even if the N–S, NNW–SSE and E–W seem to be lightly predominant.

Successively, the lineaments on the total map were color coded according to the seven trends classified above. The resulting map (Fig. 7) shows the lineament pattern colored following the recognized trends and can be utilized to discriminate the zones with a high density of sub-parallel features. These zones show the presence of more persistent (at time) lineaments which can be coinciding with faults.

6. Strike domain and fracture potential analysis

In order to discretize the information present in the compiled Lineament Map, a calculation was performed using the following procedures:

A grid was overlain on the area with 500 m grid cell size in both x and y direction; for each grid cell center, P21s [27] density was calculated using the following relationship:

$$P21s = \sum \frac{Ls}{Ac} \quad (1)$$

where P21s (1/m) is the density of the 1D element (linear features) in a 2D (area) domain, Ls (m) is the length of the part of the segment which resides within the circle defined by the search radius S , inversely scaled for distance to the cell center, Ac (m^2) is surface area of the search circle and S (m) is the radius of the search circle (for the current study $S = 1000$ m).

Furthermore for each grid cell center, a rosette was generated representing P21s values for 10 degrees of strike direction, normalized to 100%, and drawn normalized to the rosette radius ($R_s = 500$ m). Border effects of the investigated area were filtered-out by means of a special technique (using the finite elements) which compares the investigated region with the search radius. The results are presented as a Fracture Potential Contour Map (Fig. 8).

The Fracture Potential Contour Map can be interpreted as reflecting the areal variation of fracture potential or total strain. Within the Fracture Potential Contour Map, there are some areas of maximum potential that can coincide with the feature alignments described in Fig. 7.

A subsequent discretization was performed by outlining the domains where each of the fracture sets comprises a

statistically significant portion of the total range of strikes. The result of this calculation is the Fracture Domain Map (Fig. 9), where the statistical cut-off is represented by 25%; this means that in this map only the trends that perceptually exceed these values are displayed.

7. Conclusions

The DQ oil field is located in an active plate zone in Iran. Hence, structural and fracture analysis of this field should never be ignored. Undoubtedly, doing such work will significantly be helpful for identification of the most hazardous area in terms of drilling instability. In this regard, current research work attempts to provide a contour map highlighting the most critical area (i.e., total strain) for drilling. Coherency seismic attribute has successfully been used for the purpose of this study and the results obtained have shown that (1) the predominant features are the SSE–NNW and N–S trends identified as yellow and green in the rosette diagram respectively, (2) the central part of the DQ structure shows the highest concentration of segment bundles, (3) the segment bundles seem to be aligned along some lineaments oriented SE–NW and SSE–NNW, and (4) on the eastern and western margins of the map there is an anomalous concentration of segments oriented E–W. It is concluded that the coherency attribute can be used for a wide range of structural analysis and it is truly able to provide meaningful results about the most unstable regions of drilling.

Acknowledgment

The authors would like to express their appreciation and gratitude to the Iranian offshore oil company for providing data for this research.

References

- [1] B.S. Aadnoy, F. Angell-Olsen, Some effects of ellipticity on the fracturing and collapse behavior of a borehole, *Int. J. Rock Mech.* 32 (6) (1995) 621–627.
- [2] B.S. Aadnoy, C. Edland, Borehole stability of multilateral junctions, *J. Petroleum Science Eng.* 30 (3–4) (2001) 245–255.
- [3] B.S. Aadnoy, S. Ong, Introduction to special issue on borehole stability, *J. Petroleum Science Eng.* 38 (3) (2003) 79–82.
- [4] N. Morita, G. Fuh, A.D. Black, Borehole breakdown pressure with drilling fluids – I. Empirical results, *Int. J. Rock Mech.* 33 (1) (1996) 39–51.
- [5] X. Chen, C. Tan, C.M. Haberfield, Guidelines for efficient wellbore stability analysis, *Int. J. Rock Mech.* 34 (3) (1997) 418.
- [6] M. Zoback, 2007. *Reservoir Geomechanics*, Cambridge University Press.
- [7] L. Vernik, M.D. Zoback, Estimation of maximum horizontal principal stress magnitude from stress-induced well bore breakouts in the Cajon pass scientific research borehole, *J. Geophys. Res.* 97 (1992) 5109–5119.
- [8] D. Wiprut, M. Zoback, Constraining the stress tensor in the Visund field, Norwegian North Sea: application to wellbore stability and sand production, *Int. J. Rock Mech. Min. Sci.* 37 (2000) 317–336.
- [9] J.S. Bell, Practical methods for estimating in situ stresses for borehole stability applications in sedimentary basins, *J. Petrol. Sci. Eng.* 38 (2003) 111–119.
- [10] M.D. Zoback, C.A. Barton, M. Brudy, D.A. Castillo, T. Finkbeiner, B.R. Grollmund, D.B. Moos, P. Peska, C.D. Ward, D.J. Wiprut, Determination of stress orientation and

- magnitude in deep wells, *Int. J. Rock Mech. Min. Sci.* 40 (2003) 1049–1076.
- [11] P.S. Charlez, A. Onaisi, Wellbore stability: one of the most important engineering challenges when drilling smart wells in interactive drilling for fast track oilfield development, in: J. Lecourtier (Ed.), *TECHNIP*, 2001, pp. 77–102.
- [12] S. Chopral, K.J. Marfurt, Seismic attributes—a historical perspective, *Geophysics* 70 (5) (2005) 28–30.
- [13] Y. Mu, S. Cao, Seismic physical modeling and sandstone reservoir detection using absorption coefficients of seismic reflections, *J. Petrol. Sci. Eng.* 41 (2004) 159–167.
- [14] S. Chopra, Coherence cube and beyond, *First Break* (2002) 27–33.
- [15] G.A. James, J.G. Wynd, Stratigraphic nomenclature of the Iranian oil consortium agreement area, *AAPG Bull.* (1965) 71.
- [16] N.F. Sadooni, Stratigraphic sequence, MICROFACIES, and petroleum prospect of the Yamama formation, lower cretaceous, southern Iraq, *AAPG Bull.* 1 (1993) 77.
- [17] F.O. Bonneau, V. Henrion, G. Caumon, P. Renard, J. Sausse, A methodology for pseudo-genetic stochastic modeling of discrete fracture networks, *Comput. Geosci.* 56 (2013) 12–22.
- [18] Y. Ling, G. Xiangyu, S. Qianggong, H. Weisheng, Fractured reservoir prediction – a case study in the Sichuan basin, search and discovery article #10512, 2013.
- [19] G. Marta, S. William, G.F.W. Julia, Natural sealed fractures in mudrocks: a case study tied to burial history from the Barnett Shale, Fort Worth Basin, Texas, USA, *Marine and Petroleum Geology*, 2013.
- [20] J.H. McBride, R. William Keach, K. Chandler, E.L. Hannes, Testing 3D seismic attribute strategies for subtle fault mapping, search and discovery article #41232, 2013.
- [21] E. Lundberg, 2D and 3D Reflection Seismic Studies over Scandinavian Deformation Zones. Digital Comprehensive Summaries of Uppsala Dissertations from the Faculty of Science and Technology 1102. i–x, p. 57. Uppsala: Acta Universitatis Upsaliensis, 2014. ISBN 978-91-554-8817-8.
- [22] Q. Chen, S. Sidney, Seismic attribute technology for reservoir forecasting and monitoring, *Lead. Edge* 16 (5) (1997) 445–456.
- [23] D.R. Schmitt, Seismic attributes for monitoring of a shallow heated heavy oil reservoir: a case study, *Geophysics* 64 (1) (1999) 368–377.
- [24] B.S. Hart, R.S. Balch, Approaches to defining reservoir physical properties from 3-D seismic attributes with limited well control, an example from the Jurassic Smackover Formation, Alabama, *Geophysics* 65 (2) (2000) 368–376.
- [25] F.A. Neves, M.S. Zahrani, S.W. Bremkamp, Detection of potential fractures and small faults using seismic attributes, *Lead. Edge* 23 (9) (2004) 903–906.
- [26] R. Walker, C. Wong, H. Malcotti, E. Pèrez, J. Sierra, Seismic multi-attribute analysis for lithology discrimination in Ganso Field, Oficina Formation, Venezuela, *Lead. Edge* 24 (11) (2005) 1160–1166.
- [27] W.S. Dershowitz, H.H. Herda, Interpretation of fracture spacing and intensity. in: J.R. Tillerson, W.R. Wawersik (Eds.), *Proceedings of the 33rd U.S. Symposium on Rock Mechanics*, Balkema, Rotterdam, 1992, pp. 757–766.